$PM2.5$ Monitoring using Images from Smartphones in Participatory Sensing

Xiaoyang Liu*, Zheng Song*, Edith Ngai†, Jian Ma*, Wendong Wang*
*State Key Laboratory of Networking and Switching Technology, Beijing University of Posts and Telecommunications, Beijing 100876, China, Email: (tonyreginald@gmail.com, sonyyt@gmail.com, majian@mwsn.com.cn, wdwang@bupt.edu.cn)
†Department of Information Technology, Uppsala University, Uppsala, Sweden, Email:edith.ngai@it.uu.se

***Abstract*—Air pollution has become one of the most pressing environmental issues in many countries, including China. Fine-grained $PM2.5$ particulate data can prevent people from long time exposure and advance scientific research. However, existing monitoring systems with $PM2.5$ stationary sensors are expensive, which can only provide pollution data at sparse locations. In this paper we demonstrate for the first time that camera on smartphones can be used for low-cost and fine-grained $PM2.5$ monitoring in participatory sensing. We propose a Learning-Based method to extract air quality related features from images taken by smartphones. These image features will be used to build the haze model that can estimate $PM2.5$ concentration depending on the reference sensors. We conducted extensive experiments over six months with two datasets to demonstrate the performance of the proposed solution using different models of smartphones. We believe that our findings will give profound impact in many research fields, including mobile sensing, activity scheduling, haze data collection and analysis.**

I. Introduction

Air pollution has been a serious concern in many developing countries such as China. Various types of pollution have increased as the country becomes more industrialized, which has caused widespread environmental and health problems. Measurements in January 2013 showed that the density of particulate matter smaller than 2.5 micrometres was literally off the chart − higher than the maximum 755 $\mu g/m^3$ that was measurable by the sensors in Beijing.

Real-time air quality monitoring is very useful for scientists and citizens to control air pollution and protect human health [1]. In the past decade, many studies highlighted the impact of ambient airborne particulate matter (PM), especially $PM2.5$, as a critical pollutant leading to different cardiopulmonary diseases and lung cancer. Providing real-time $PM2.5$ measurements can help people to schedule their daily routines to avoid exposure to airborne carcinogens.

However, existing $PM2.5$ monitoring systems often fail to provide fine-grained measurements in large area due to the high hardware cost. Take Beijing as an example, only 22 stationary sensors are deployed to collect $PM2.5$ data (see Fig.1). Considering Beijing with an area of 4,055,000 acres, the sparse distribution of sensors can provide only coarse measurements in the city. Nevertheless, deploying large amount of sensors is not feasible, since high quality $PM2.5$ sensors cost tens of thousands of dollars and are hard to be maintained.

Since stationary $PM2.5$ sensors are expensive, we have been thinking of utilizing low quality portable sensors carried by mobile users. One issue is that existing smartphones are not equipped with pollution sensors. Although external $PM2.5$ sensors can be considered, they are costly, inaccurate, and inconvenient to bring around. In the meantime, many people take photos and publish them through social network these days. We observe that the photos taken at the same place may look quite differently depending on the air quality of the day (see Fig.2 as an example). This inspires us to exploit the potential of using smartphone photos to estimate $PM2.5$ concentration around the city.

In this paper, we propose a novel approach to infer $PM2.5$ concentration from photos taken by smartphones. Based on lightweight image processing techniques, a participatory sensing system for air pollution monitoring can be built without any additional hardware to the smartphones. We investigate the relationship between the haze model [2] and the image, in which relevant features are extracted to estimate the haze model. Based on the haze model, we further deduce the $PM2.5$ concentration according to the physics models [3].

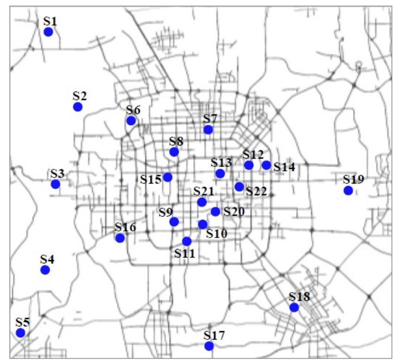

Fig. 1: Air quality measurement stations in Beijing

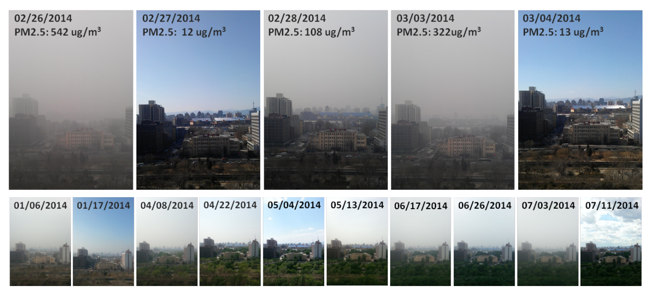

Fig. 2: Photos taken in Beijing from Jan to Jul 2014

978-1-4673-7131-5/15/$31.00 ©2015 IEEE

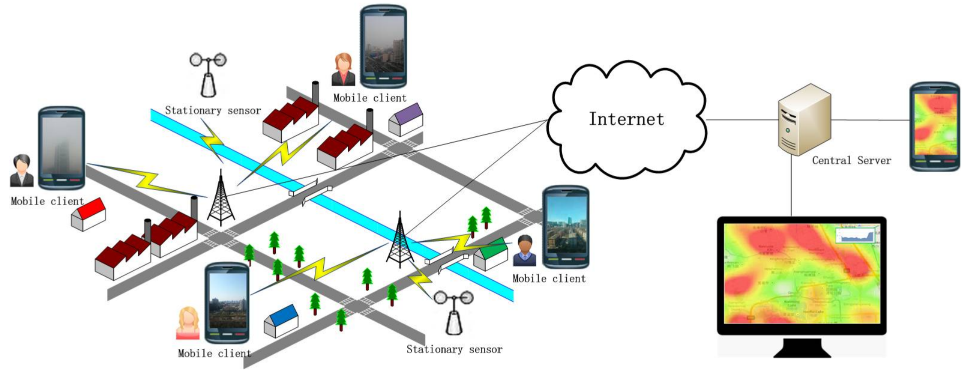

Fig. 3: System architecture

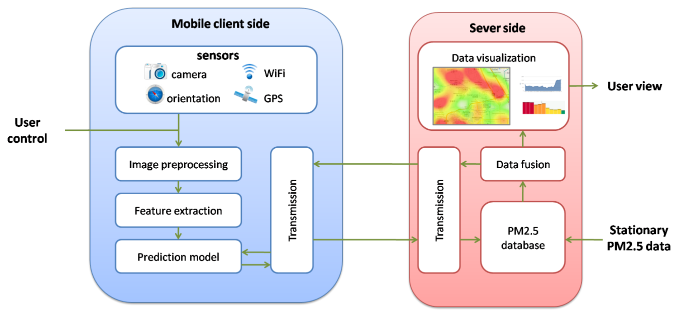

Fig. 4: Data flow of the system

Our participatory sensing system enables mobile users to take photos, estimate $PM2.5$ concentration, and share their results with other people in the city.

The main contribution of this paper is threefold:

1) To the best of our knowledge, we are the first to propose and develop a participatory sensing system that enables mobile users to estimate $PM2.5$ concentration from photos taken by their smartphones. It provides a low-cost and fine-grained solution for monitoring $PM2.5$ concentration in wide area utilizing the sensing and computing capability of the mobiles.

2) We propose a Learning-Based (LB) method to estimate $PM2.5$ concentration. The LB method can infer $PM2.5$ concentration accurately utilizing readings from nearby reference sensors to train the prediction model.

3) We collected 2 datasets using different smartphones in different places with each dataset containing 3-month photos and corresponding $PM2.5$ readings in Beijing. We also implemented the $PM2.5$ participatory sensing system, and conducted extensive experiments on the datasets to evaluate its accuracy with different smartphones in different places. The experiment results demonstrated that our system can achieve nearly 90% accuracy in $PM2.5$ estimation compared with the ground truth.

The rest of this paper is organized as follows: Section II presents the related work. Section III describes the design of our participatory sensing system for $PM2.5$ estimation. Section IV introduces the image features that are relevant to the haze model and $PM2.5$ estimation. Section V describe our proposed LB method for $PM2.5$ estimation. Section VI explains the implementation and results of the experiments. Section VII concludes this paper with future work.

II. Related Work

Pollution monitoring has been widely studied in wireless sensor networks. For example, AirCloud [4] has been proposed as a $PM2.5$ monitoring system using particulate matter monitors to infer $PM2.5$ concentration. With the popularity of mobile phones, participatory sensing is considered to be a novel approach for urban sensing [5], [6]. Several projects have utilized mobile phones with other external sensors to monitor air pollution, such as carbon monoxide (CO), nitrogen dioxide (NO_2), and ozone (O_3) [7], [8]. Mobile phones with external sensors can capture fine-grained air quality in the city, but they are costly and bulky for ordinary users.

As camera becomes a standard component on smartphone, different approaches have been proposed to measure atmospheric visibility from images. For example, Kim et al. [9] used HSI color difference to estimate the visibility of the scene. In addition, spatial contrast, frequency contrast and dark channel have been explored to estimate visibility and light extinction [10], [11]. The above work used high resolution digital cameras to capture images at fixed locations. Nevertheless, the impact and feasibility of using cameras on smartphones for visibility estimation remains to be further explored. S. Poduri et al. [12] used sky luminance to estimate air turbidity using mobile phones. The users are asked to select a small area of the sky. Then, the air quality is estimated by comparing the intensity of the selected sky area with the sky luminance model. However, this approach suffers badly from the low sensibility of the camera and does not work on a cloudy day.

III. $PM2.5$ Participatory Sensing System

Figure 3 shows the network architecture of the proposed $PM2.5$ participatory sensing system. It consists of a number of mobile devices and a server in the cloud. Stationary $PM2.5$ sensors will also be connected to the server, so that their readings can be used to train the prediction model and thereby increasing data accuracy. The mobile users take photos using their mobile devices equipped with cameras, which will be used later for $PM2.5$ estimation. The mobile devices can communicate with the server through 3G or Wifi. The server collects the estimated $PM2.5$ results from the participants, and uses data fusion methods to create a map of $PM2.5$ measurements in the city.

Figure 4 shows the detailed data flow of the system. The basic flow of $PM2.5$ estimation includes the following steps:

1) *Data Collection*: Original data such as photos, orientation data and GPS locations are collected by the mobile devices.
2) *Feature Extraction*: Image features such as spatial contrast, HSI color difference and dark channel of the images are extracted from the original photos using image processing techniques. We will discuss how to extract those features in Section IV. We explore lightweight feature extraction techniques that can be carried out locally on the mobiles to reduce communication overhead.
3) *Modelling*: The mobile client communicates with the server to obtain $PM2.5$ readings from the nearest stationary sensor and build up the $PM2.5$ estimation model. A Learning-Based (LB) method is proposed to estimates $PM2.5$ concentration using a series of photos and readings from nearby stationary $PM2.5$ sensor for training the model.
4) $PM2.5$ *Estimation and Upload*: Based on the $PM2.5$ estimation model and the extracted features, $PM2.5$ estimation can be carried out on the mobile client. The estimated $PM2.5$ readings are then uploaded to the server. The server aggregates all the uploaded $PM2.5$ estimations and creates a fine-grained $PM2.5$ map of the city for visualization.

IV. Preliminary

We exploit the possibility of estimating $PM2.5$ concentration through participatory sensing with smartphone photos. This relies on the image quality and the processing techniques for feature extraction on smartphones. We use M_f to denote the $PM2.5$ concentration estimated by a smartphone. Three key image features, including the spatial contrast, the dark channel, and the HSI color difference, are extracted from the photos. Here, we first explain how these image features are related to the haze model, and then show how to use these features to estimate $PM2.5$ concentration.

A. How to Estimate $PM2.5$ from Haze Model?

Haze is an atmospheric phenomenon where dust, smoke and other dry particulates (e.g. $PM2.5$) obscure the clarity of the sky, which may make image blurry and brownish. The level of degradation of the image can be used to build the haze model, and then to estimate the $PM2.5$ concentration.

In theory, the relationship between the image and the meteorological parameters of the haze model can be expressed by an optical model [13] with

$$I(x) = J(x)t(x) + A(1 - t(x)), \tag{1}$$

where x is the 2D spatial position of the image, $J(x)$ is scene irradiance, and A represents the global atmospheric light. $I(x)$ is the observed image irradiance. Note that the image irradiance is not the final image intensity that we get from the photo, since different cameras will apply different non-linear mappings from the observed image irradiance to the image intensity in each pixel [14]. $t(x)$ is an important meteorological parameter called transmission, which indicates how much light can pass through the atmosphere. $t(x)$ ranges from 0 to 1, which can be expressed by

$$t(x) = e^{-\beta d(x)}, \tag{2}$$

where β is the light extinction and $d(x)$ is the scene depth that shows the distance between the object in the image and the mobile user.

Since $PM2.5$ particulate is a major contributor to light extinction [3], we plan to estimate the $PM2.5$ concentration, M_f, based on the light extinction, β, using the theoretical model proposed by [3].

$$\beta \approx pM_f, \tag{3}$$

$$t(x) = e^{-pd(x)M_f}, \tag{4}$$

where p is a constant and set to 3.75 in urban area in the theoretical model. Note that some special weather conditions like rain, snow, fog may introduce random spatial and temporal variations in images and hence must be dealt with differently from clear weathers [2]. In this work, the $PM2.5$ estimation algorithm only works under more common weathers (e.g. sunny, cloudy) in Beijing.

We will use both Eq. (1) and Eq. (4) to estimate the $PM2.5$ concentration. They are applied in different ways according to the types of image features.

B. Image Features

We explore the following three image features that are mostly relevant to the haze model. These include the spatial contract (F_{sc}), the dark channel (F_{dc}), and the HSI color difference of the sky (F_{hsi}). These features will be use to estimate the $PM2.5$ concentration, M_f.

1) Spatial Contrast (F_{sc}): The degradation of image caused by haze can be observed from the decrease of image contrast. As shown in Fig. 2, distant objects in images with haze lose acuity. The magnitude of the image gradient can be used to define the image contrast F_{sc} [10]. For a small block of an image, we can assume that the depth $d(x)$, the global atmospheric light A, and the concentration of the particles M_f are constant. We take gradient magnitude on both sides in Eq. (1).

$$\begin{aligned} &F_{sc} = |\nabla_x I(x)| = |\nabla_x (J(x)t(x) + A(1 - t(x)))| \\ &= t(x)|\nabla_x (J(x))| \\ &= e^{-pd(x)M_f}|\nabla_x (J(x))|. \end{aligned} \tag{5}$$

By taking log on both sides in Eq. (5) and rearranging the equation, we get

$$M_f = -\frac{1}{pd(x)}\ln(F_{sc}) + \frac{1}{pd(x)}\ln(|\nabla_x J(x)|), \tag{6}$$

where M_f and $\ln(F_{sc})$ are linear. In this work, we apply the Sobel filter f_{sobel} on $I(x)$ to measure the gradient magnitude of the image. Then, we have

$$F_{sc} = f_{sobel}(I(x)). \tag{7}$$

2) Dark Channel (F_{dc}): The dark channel feature, recently proposed by He [13], has been widely used in haze removal. It is based on the assumption that there is at least one color channel including pixels with very low or close to zero intensity in most of the non-sky blocks of the image. The dark channel of an image is defined by

$$J_{dark}(x) = \min_{y\in\Omega(x)} \left\{ \min_{c\in\{r,g,b\}} J^c(y) \right\}, \tag{8}$$

where J^c is one color channel of the scene radiance J and $\Omega(x)$ is a small block around the pixel x. From the equation, we can see that the dark channel value of a given pixel is the minimum intensity of the three color channels of the image block around it. From He's observation, the dark channel of a haze-free image should be zero. It is also called dark channel prior, which has the property of

$$J_{\mathrm{dark}} \to 0. \tag{9}$$

By applying dark channel prior to Eq. (1), we can get the estimated transmission $\tilde{t}(x)$ of the image by

$$\tilde{t}(x) = 1 - \min_{y\in\Omega(x)} \left\{ \min_{c} \frac{I^c(y)}{A^c} \right\}, \tag{10}$$

where A^c is the estimated global atmospheric light. A^c is picked from the highest intensity of the image, such as the brightest 0.1 percent of the pixels in the dark channel. From Eq. (4), we find that there is an exponential relationship between the estimated $\tilde{t}(x)$ and the $PM2.5$ concentration. Thus, we choose $\tilde{t}(x)$ as an image feature, denoted by F_{dc}, and obtain

$$M_f = -\frac{1}{pd(x)} \ln(F_{dc}). \tag{11}$$

3) HSI Color Difference of Sky (F_{hsi}): The above two features both make use of the non-sky area to estimate $PM2.5$ concentration. In fact, the sky area of an image can also be used for $PM2.5$ estimation. The HSI color difference of sky taken under different weather changes with the visibility and the hazy conditions (as shown in Fig.2). It has been proven that the HSI color difference has an exponential relation with the light extinction [12], which can be modelled by

$$\beta = a e^{b\Delta D}, \tag{12}$$

where a and b are coefficients of the model, and ΔD is the HSI color difference. If we take a sky image on a clear (haze-free) day as a reference, the HSI color difference of a target sky image is

$$F_{hsi} = \Delta D = \sqrt{(\Delta H)^2 + (\Delta S)^2 + (\Delta I)^2}, \tag{13}$$

where ΔH, ΔS, ΔI are the hue, saturation, intensity difference between the target and the reference [12]. From Eq. (3) and Eq. (12), we can then obtain

$$M_f = \frac{a}{p} e^{bF_{hsi}}. \tag{14}$$

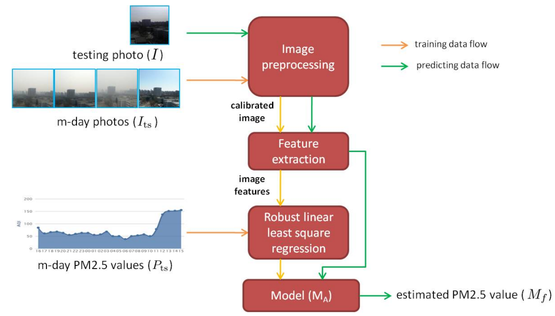

Fig. 5: Framework of client side for the LB approach

V. The LB Approach

An overview of the Learning-Based (LB) approach is shown in Fig. 5. The mobile user is required to take a sequence of photos, $I_{\mathrm{ts}}=\{I_{ts}^1, I_{ts}^2, I_{ts}^3, \cdots, I_{ts}^m\}$, at the same place for m days (see example in Fig. 2) to build a prediction model using the $PM2.5$ data, $P_{\mathrm{ts}}=\{P_{ts}^1, P_{ts}^2, P_{ts}^3, \cdots, P_{ts}^m\}$, measured by the nearest $PM2.5$ station as ground truth. By running image feature extraction and supervised learning algorithm on the client side, we can establish a prediction model $Model_{LB}$ for one place using I_{ts} and P_{ts}. Afterwards, given a new photo I taken at the same place, we can acquire the estimated $PM2.5$ concentration, M_f, using the prediction model as

$$M_f = Model_{LB}\left(I, I_{ts}, P_{ts}\right). \tag{15}$$

A. Image Preprocessing

Image preprocessing is needed before feature extraction for two reasons. First, data filtering is required to exclude invalid photos which may cause significant errors in the estimation result. For example, a photo taken in rain or snow can not be used to estimate $PM2.5$ concentration since it generates random interference to the haze model [2]. We will ignore photos taken in poor weather conditions. To accomplish this, local weather data will be obtained from the Internet. Second, as mentioned above, $I(x)$ in Eq. (1) is the observed image irradiance of pixel x. However, the imaging system of smartphone camera often applies a non-linear mapping of the observed image irradiance to the brightness of each pixel. This transformation is called the camera response function [14], which needs to be learned in order to recover the image irradiance. We adopt a radiometric calibration method proposed by [15], which uses a single image to estimate camera response function based on linear RGB distribution at color edges.

B. Feature Extraction

We use the three image features, F_{sc}, F_{dc} and F_{hsi}, described in Section IV to estimate the $PM2.5$ concentration. Note that we need only one of these features to perform $PM2.5$ estimation.

C. $PM2.5$ Estimation

Both the ground truth $PM2.5$ data, P_{ts}, and the features extracted from I_{ts} will be used to train the prediction model, $Model_{LB}$. By employing robust linear least square regression

TABLE I: Details of the datasets

Data sources	Dataset 1	Dataset 2
Location	Scene 1: campus T3 Building	Scene 2: BTV building
Orientation	west	west
Cameras	Samsung S3 , HTC G14	digital camera
Capture time	14:00	8:00
Time span	2/27/2014 - 5/13/2014	10/1/2013 - 1/30/2014
Image size	1152 × 2048	560 × 600
Data size	100	100

on the features, F_{sc} and F_{dc}, we can learn the coefficients in Eq. (6) and Eq. (11). Similarly, by applying non-linear least square regression on feature F_{hsi}, we can obtain the coefficients in Eq. (14). After that, we can use the extracted features to estimate $PM2.5$ concentration. Take feature F_{sc} as an example, we can estimate parameters w_0 and w_1 according to Eq. (6), i.e. $M_f = w_1 \ln(F_{sc}) - w_0$. For a given F_{sc} value, we can then calculate the estimated M_f value.

It is worth mentioning that not all areas in the image are effective for $PM2.5$ concentration. For example, objects that are too far or too close using features F_{sc} and F_{dc}, or ground objects using feature F_{hsi} may lead to significant errors in $PM2.5$ estimation. Therefore, we develop a sliding window approach to determine the best area of the image that gives the highest correlation between the image features and the $PM2.5$ concentration. Then, we use only the feature value in the best area to estimate $PM2.5$ concentration.

From our experiment, we found that F_{dc} is much more effective than F_{sc} and F_{hsi}. We will show the accuracy of these image features for $PM2.5$ estimation in Section VI. Following this finding, we make use of the F_{dc} feature to perform $PM2.5$ estimation in the LB approach.

VI. Experiments

In this section, we implement the PM2.5 participatory sensing system and conduct extensive experiments to evaluate its performance. First, we describe the datasets and evaluation metrics that we used in our experiments. Then, we present the experiment results and analysis of the LB approach.

A. Experiment Settings

1) Datasets: We evaluate our system using two sets of images collected at different locations. We use the $PM2.5$ readings published by different $PM2.5$ monitor stations in Beijing [16], [17] as ground truth.

a) Image Data: The image data consists of 200 photos taken over 6 months in Beijing as summarized in Table I. Most of the weather conditions in photos are sunny or cloudy, which are the most common weathers in Beijing. Datasets 1 is collected by ourselves at different buildings and orientations in campus, which is close to S_8 station (see Fig.1). The photos were captured by ourselves using two different smartphone models (Samsung S3 and HTC G14) at the same time everyday for nearly three months. In order to evaluate our approach at a different location, dataset 2 is also used in our experiment. It contains a set of images collected by Y. Zou [18] over four months in the BTV building, which is near to S_{22} station (see Fig.1).

b) Ground Truth Data: The $PM2.5$ readings reported by the stations in Beijing are used as the ground truth to train the prediction model and evaluate the estimation results in the LB approach.

2) Evaluation Metrics: We use the coefficient of determination (R^2) between the estimated $PM2.5$ concentration and the ground truth data to evaluate the accuracy of the estimation. Let p'_i and p_i be the ith estimated $PM2.5$ value and the corresponding ground truth $PM2.5$ data in the testing set. R^2 can be calculated by

$$R^2 = 1 - \frac{\sum_{i=1}^{n} (p'_i - p_i)^2}{\sum_{i=1}^{n} (p_i - \bar{p})^2}, \tag{16}$$

where n is the size of the testing set and $\bar{p}$ is the mean of ground truth data in the testing set, and R^2 ranges from 0 to 1. Higher R^2 value indicates higher accuracy of our prediction model. In addition, we calculate the mean absolute error (MAE) between the estimated $PM2.5$ concentration and the ground truth by

$$MAE = \frac{1}{n} \sum_{i=1}^{n} |p'_i - p_i|. \tag{17}$$

B. $PM2.5$ Estimation Accuracy

Table II summarizes the experimental results of R^2 and MAE for the three image features, including spatial contrast (F_{sc}), dark channel (F_{dc}), and HSI color difference (F_{hsi}). We observe that F_{dc} achieves the highest R^2 and the lowest MAE compared with the other two features. It performs the best in all scenes regardless of the types of mobile phones in our experiment. In contrast, F_{hsi} has the worst performance among the three features. We find that it suffers seriously from the cloud in the sky. This phenomenon leads to significant error in the HSI color difference and results in poor performance of the prediction model.

Fig. 6 compares the estimated $PM2.5$ concentration with the ground truth in Scene 1 (using smartphones) and Scene 2 (using digital camera). We find that the $PM2.5$ estimation result is closer to the ground truth in Scene 1 than in Scene 2. This may be due to the low resolution of the camera in dataset 2. We also notice that the estimated $PM2.5$ values using HTC G14 are often slightly higher than the ground truth in Scene 1. On the contrary, the estimated $PM2.5$ concentration values using digital camera are often underestimated compared with the ground truth in Scene 2. We believe that this is due to an offset error from image processing, such as inaccuracy of radiometric calibration in the preprocessing step.

Next, we investigate the accuracy of $PM2.5$ estimation varying the size of training set, m. Intuitively, the larger m is, the more accurate our prediction model and the longer the training time. Fig. 7 shows the performance of our prediction model in the LB approach varying m from 3 to 20. When m increases, R^2 increases and MAE decreases with less fluctuation. R^2 tends to be stabilized when m is greater than 15. This result implies that half-month of training data is

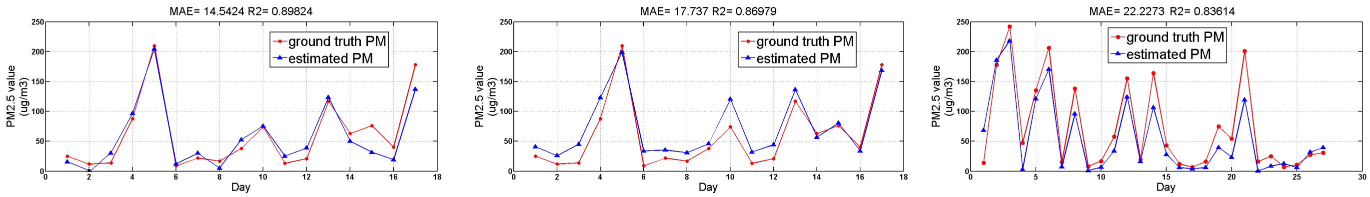

(a) Scene 1 using Samsung S3 (b) Scene 1 using HTC G14 (c) Scene 2 using digital camera

Fig. 6: $PM2.5$ estimation results using feature F_{dc} in the LB approach

enough to build the prediction model accurately for $PM2.5$ estimation. From this result, we choose m to be 15 in our system.

TABLE II: Summary of performance evaluation for the LB approach

Features	Scene 1				Scene 2	
	HTC G14		Samsung S3		Digital Camera	
	MAE	R^2	MAE	R^2	MAE	R^2
F_{sc}	27.18	0.8463	27.06	0.8014	31.06	0.6662
F_{dc}	17.73	0.8689	14.54	0.8982	22.23	0.8361
F_{hsi}	33.52	0.7155	30.56	0.6996	32.23	0.6801

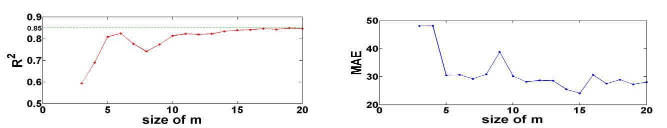

(a) R^2 in Scene 1 using HTC G14 (b) MAE in Scene 1 using HTC G14

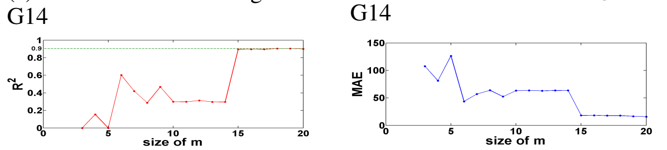

(c) R^2 in Scene 1 using Samsung S3 (d) MAE in Scene 1 using Samsung S3

Fig. 7: Performance of the LB approach varying m

VII. Conclusions and Future Work

In this paper, we proposed for the first time a feasible solution for $PM2.5$ monitoring using camera on smartphones through participatory sensing. It utilizes images taken by mobile users in the city to provide real-time and fine-grained $PM2.5$ concentration estimation at low cost. We designed and implemented the $PM2.5$ monitoring system in a distributed fashion leveraged the computation capability of the smartphones. The LB approach is proposed to estimate $PM2.5$ using a series of user's photos. We have conducted extensive experiments using different models of smartphones in different places for six months. The experiment results demonstrated that our system can achieve close to 90% accuracy in $PM2.5$ estimation compared with the ground truth.

For future work, we will open our system to the public and conduct more experiments in different cities. We would also like to investigate the impact of different weathers and seasons in the system, since our system can not work when it rains or snows. Other factors like $PM10$ or fog need to be further investigated in $PM2.5$ estimation. In addition, we plan to explore incentive mechanism [19] to motivate participants take photos everyday in the LB approach, as well as privacy protection mechanism [6] and energy-preserving methods [20] to improve our system.

References

[1] Y. Zheng, F. Liu, and H.-P. Hsieh, "U-air: when urban air quality inference meets big data," in *ACM SIGKDD '13*, pp. 1436–1444.

[2] S. K. Nayar and S. G. Narasimhan, "Vision in bad weather," in *IEEE ICCV '99*, vol. 2, pp. 820–827.

[3] H. Ozkaynak, A. D. Schatz, G. D. Thurston, R. G. Isaacs, and R. B. Husar, "Relationships between aerosol extinction coefficients derived from airport visual range observations and alternative measures of airborne particle mass," *Journal of the Air Pollution Control Association*, vol. 35, no. 11, pp. 1176–1185, 1985.

[4] Y. Cheng, X. Li, Z. Li, S. Jiang, Y. Li, J. Jia, and X. Jiang, "Aircloud: A cloud-based air-quality monitoring system for everyone," in *ACM SenSys '14*, pp. 251–265.

[5] M. Musthag and D. Ganesan, "Labor dynamics in a mobile micro-task market," in *ACM SIGCHI '13*, pp. 641–650.

[6] X. Chen, X. Wu, X.-Y. Li, Y. He, and Y. Liu, "Privacy-preserving high-quality map generation with participatory sensing," in *IEEE INFOCOM '14*, pp. 2310–2318.

[7] B. Predic, Z. Yan, J. Eberle, D. Stojanovic, and K. Aberer, "Exposuresense: Integrating daily activities with air quality using mobile participatory sensing," in *IEEE PERCOM Workshops '13*, pp. 303–305.

[8] N. Nikzad, N. Verma, C. Ziftci, E. Bales, N. Quick, P. Zappi, K. Patrick, S. Dasgupta, I. Krueger, T. Š. Rosing *et al.*, "Citisense: improving geospatial environmental assessment of air quality using a wireless personal exposure monitoring system," in *Proceedings of the ACM conference on Wireless Health '12*, pp. 11:1–11:8.

[9] S. Poduri, A. Nimkar, and G. S. Sukhatme, "Visibility monitoring using mobile phones," *Annual Report: Center for Embedded Networked Sensing*, pp. 125–127, 2010.

[10] N. Graves and S. Newsam, "Using visibility cameras to estimate atmospheric light extinction," in *IEEE WACV '11*, pp. 577–584.

[11] L. Xie, A. Chiu, and S. Newsam, "Estimating atmospheric visibility using general-purpose cameras," in *Advances in Visual Computing*, vol. 5359. Springer, 2008, pp. 356–367.

[12] K. W. Kim and Y. J. Kim, "Perceived visibility measurement using the hsi color difference method," *Journal of the Korean Physical Society*, vol. 46, no. 5, pp. 1243–1250, 2005.

[13] K. He, J. Sun, and X. Tang, "Single image haze removal using dark channel prior," *IEEE PAMI*, vol. 33, no. 12, pp. 2341–2353, 2011.

[14] M. D. Grossberg and S. K. Nayar, "What is the space of camera response functions?" in *IEEE CVPR '03*, vol. 2, pp. 602–609.

[15] S. Lin, J. Gu, S. Yamazaki, and H.-Y. Shum, "Radiometric calibration from a single image," in *IEEE CVPR '04*, vol. 2, pp. 938–945.

[16] "Beijing municipal environmental monitoring center," http://zx.bjmemc.com.cn/, 2014.

[17] "Twitter of Beijing US embassy," https://twitter.com/BeijingAir/, 2014.

[18] "Photos provided by Y. Zou," http://weibo.com/p/1005051000481815/, 2014.

[19] I. Koutsopoulos, "Optimal incentive-driven design of participatory sensing systems," in *IEEE INFOCOM '13*, pp. 1402–1410.

[20] Q. Zhao, Y. Zhu, H. Zhu, J. Cao, G. Xue, and B. Li, "Fair energy-efficient sensing task allocation in participatory sensing with smartphones," in *IEEE INFOCOM '14*, pp. 1366–1374.